Available online at www.sciencedirect.com
ScienceDirect
Ceramics International 34 (2008) 273–278
CERAMICS INTERNATIONAL
www.elsevier.com/locate/ceramint

Synthesis and microstructure of (LaSr)MnO_3 and (LaSr)FeO_3 ceramics by a reaction-sintering process

Yi-Cheng Liou *, Yow-Renn Chen

Department of Electronics Engineering, Kun-Shan University, Tainan Hsien, 71003 Taiwan, ROC

Received 28 July 2006; received in revised form 22 August 2006; accepted 5 September 2006
Available online 28 November 2006

Abstract

$(La_xSr_{1-x})MnO_3$ (LSMO) and $(La_xSr_{1-x})FeO_3$ (LSFO) ($x = 0.2$–0.4) ceramics prepared by a simple and effective reaction-sintering process were investigated. Without any calcination involved, La_2O_3 and $SrCO_3$ were mixed with MnO_2 (LSMO) or Fe_2O_3 (LSFO) then pressed and sintered directly. LSMO and LSFO ceramics were obtained after 2 and 4 h sintering at 1350–1400 and 1200–1280 °C, respectively. Grain size decreased as La content increased in LSMO and LSFO ceramics.

Keywords: $(La_xSr_{1-x})MnO_3$; $(La_xSr_{1-x})FeO_3$; Reaction-sintering process; Microstructure

1. Introduction

Perovskite-type oxides $LnMO_3$ (Ln = lanthanide elements; M = transition metals) have received much attention because their applications in solid-oxide fuel cells (SOFC) [1–4] and sensor materials for alcohol, carbon monoxide, oxygen, and humidity [5–8]. SOFCs are energy-conversion devices and contain three parts, including the electrolyte, the anode and the cathode. A dense electrolyte is needed to prevent gas mixing, whereas the anode and cathode must be porous to allow gas transport to the reaction sites. Mixed ionic-electronic conductors $(La_xSr_{1-x})MnO_3$ (LSMO) and $(La_xSr_{1-x})FeO_3$ (LSFO) are receiving great attention as cathode and interconnection materials for SOFCs [9–13]. LSMO and LSFO ceramics are conventionally prepared by solid-state reaction process, calcining and sintering at high temperatures are involved. Bilger et al. produced LSMO via a sol–gel method [14]. Licci and co-workers obtained LSMO from the mixed citrate precursors [15]. Perovskite-type LSMO powders were synthesized via a mechanochemical process by grinding the constituent oxides using a planetary mill in air by Zhang et al. [16]. Simner and co-workers synthesized LSFO via a glycine nitrate combustion technique [17].

Recently, Liou et al. prepared $Pb(Mg_{1/3}Nb_{2/3})O_3$ (PMN) and $Pb(Fe_{1/2}Nb_{1/2})O_3$ (PFN) ceramics by a simple and effective reaction-sintering process [18,19]. PbO and Nb_2O_5 were mixed with $Mg(NO_3)_2$ or $Fe(NO_3)_3$ then pressed and sintered directly into PMN and PFN ceramics with the calcination step bypassed. These are the first successful synthesis of perovskite relaxor ferroelectric ceramics without having to go through the calcination step in the conventional mixed oxide route or in the columbite/wolframite route (two calcination steps were involved). PMN ceramics with a density 8.09 g/cm^3 and dielectric constant 19,900 (1 kHz) were obtained. Other Pb-based complex perovskite ceramics were also produced by this reaction-sintering process successfully. In recent studies, some microwave dielectric ceramics such as $BaTi_4O_9$, $(Ba_xSr_{1-x})(Zn_{1/3}Nb_{2/3})O_3$, $Ba_5Nb_4O_{15}$, $Sr_5Nb_4O_{15}$, $CaNb_2O_6$ and $NiNb_2O_6$ were also prepared successfully by this reaction-sintering process [20–24]. In this study, we try to prepare $(La_xSr_{1-x})MnO_3$ and $(La_xSr_{1-x})FeO_3$ ceramics by a reaction-sintering process.

2. Experimental procedure

All samples in this study were prepared from reagent-grade oxides: La_2O_3 (99.9%), $SrCO_3$ (99%), MnO_2 (99.9%) and Fe_2O_3 (99.9%). Appropriate amounts of raw materials for stoichiometric $(La_xSr_{1-x})MnO_3$ and $(La_xSr_{1-x})FeO_3$ ($x = 0.2$, 0.25, 0.3, 0.35 and 0.4) were milled in distilled water with

* Corresponding author. Tel.: +886 6 2050521; fax: +886 6 2050250.
E-mail address: ycliou@mail.ksu.edu.tw (Y.-C. Liou).

0272-8842/$34.00
doi:10.1016/j.ceramint.2006.09.015

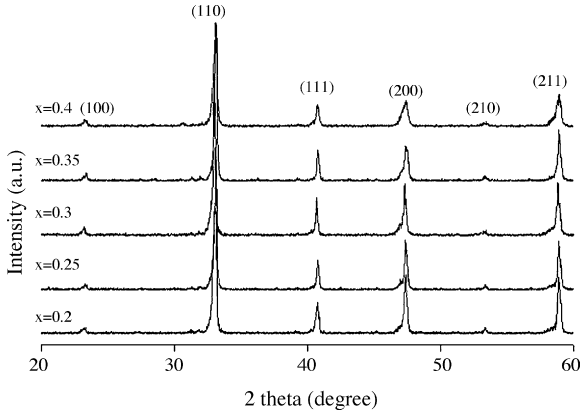

Fig. 1. XRD profiles of LSMO ceramics sintered at 1350 °C for 2 h.

alumina balls for 24 h. After the slurry was dried and pulverized the powder was pressed into pellets 12 mm in diameter and 1–2 mm thick. The pellets were then heated at a rate 10 °C/min and sintered in a covered alumina crucible for 2 and 4 h in air at temperatures 1350–1400 °C for LSMO and 1200–1280 °C for LSFO.

The density of sintered pellets was measured by the Archimedes method. The sintered LSMO and LSFO ceramics were analyzed by X-ray diffraction (XRD) to check the reflections of the phases. Microstructures were analyzed by scanning electron microscopy (SEM).

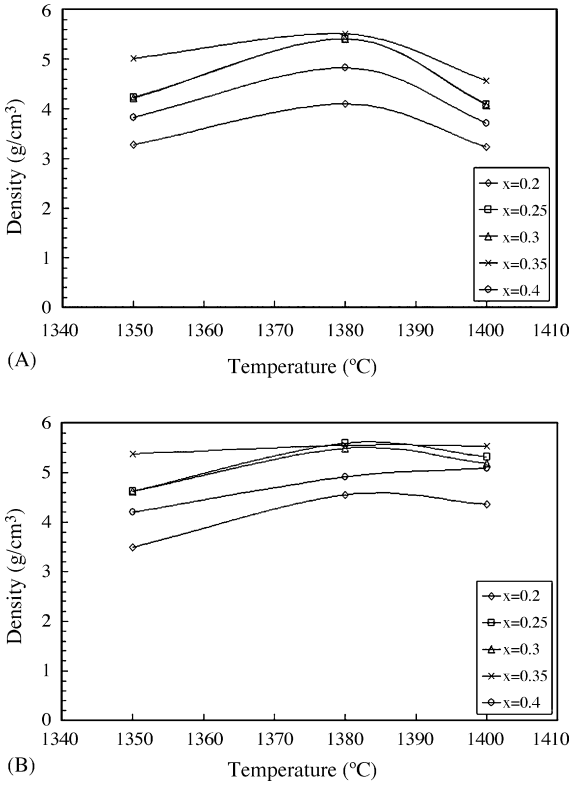

Fig. 2. Density of LSMO ceramics sintered at various temperatures for (A) 2 h and (B) 4 h.

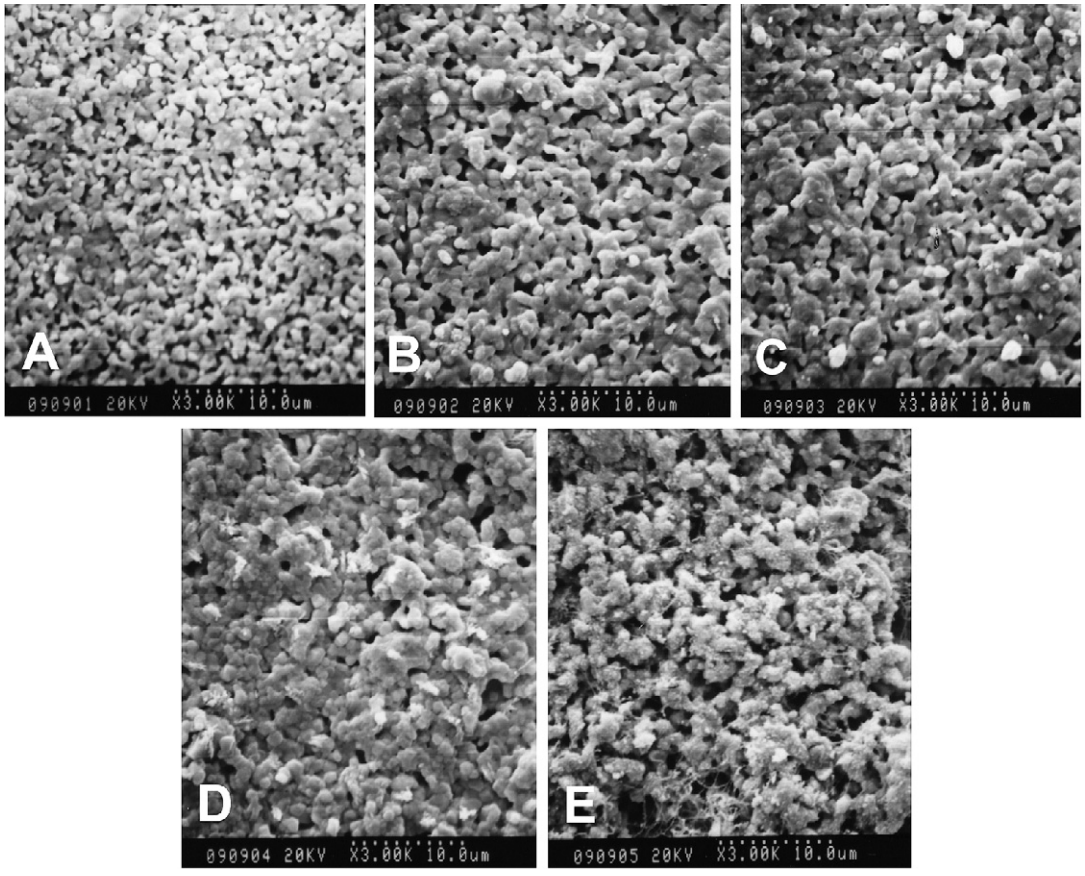

Fig. 3. SEM photographs of the as-fired $(La_xSr_{1-x})MnO_3$ ceramics with (A) $x = 0.2$, (B) $x = 0.25$, (C) $x = 0.3$, (D) $x = 0.35$ and (E) $x = 0.4$ after 1350 °C/2 h sintering.

3. Results and discussion

Fig. 1 shows XRD profiles of LSMO ceramics prepared by the reaction-sintering process. All peaks match well with the standard pattern. LSMO ceramics could be obtained successfully by a simple process even with the calcining stage bypassed. Therefore, the reaction-sintering process is proven effective in preparing LSMO ceramics. The density values of LSMO sintered at various temperatures are shown in Fig. 2. It increases with sintering temperature and reaches a maximum value at 1380 °C in 2 h sintering LSMO. It also increased with La content till $x = 0.35$ then decreased obviously at $x = 0.4$. The maximum density occurred at 1400 °C for 4 h sintering LSMO with $x = 0.35$ and 0.4.

SEM photographs of as-fired LSMO ceramics sintered at 1350 °C/2 h are shown in Fig. 3. Porous pellets with fine grains about 1 μm were formed in these LSMO ceramics. This means that 1350 °C/2 h sintering is not high enough for grain growth and densification in LSMO ceramics prepared by the reaction-sintering process. It can be easily observed that pores decreased as the La content increased at $x = 0.2$–0.35 and increased again at $x = 0.4$. Similar trend was observed in LSMO ceramics prepared by the conventional mixed oxide route [25]. SEM photographs of the as-fired LSMO ceramics sintered at 1380 °C/2 h are illustrated in Fig. 4. Pores are still found in LSMO ceramics with $x = 0.2$ and deceased obviously at $x = 0.25$. Increased porosity is needed in a cathode of SOFC to increase the gas transported to the reaction sites in the electrolyte. Larger grains were formed in LSMO prepared by the reaction-sintering process as compared with LSMO prepared by the conventional mixed oxide route [25]. It is also noted that the grain size decreased as La content increased. This is the same as in LSMO, $(La_xSr_{1-x})CoO_3$, LSFO ceramics by the conventional mixed oxide route we investigated and in $La_{1-x}Sr_xCo_{0.2}Fe_{0.8}O_3$ ceramics reported by Chou and co-workers. In LSMO by the conventional route, grains of 1.9 and <0.8 μm were found after 1400 °C/4 h sintering with $x = 0.25$ and 0.4, respectively [25]. While in LSFO ceramics by the conventional route, 6.1 μm grains were formed for $x = 0.2$ and 2.4 μm for $x = 0.4$ at 1250 °C/4 h sintering [26]. Chou et al. reported mean grain size of $La_{1-x}Sr_xCo_{0.2}Fe_{0.8}O_3$ ceramics increased about 12 times from 1.8 μm for 80% La content to 21.9 μm for 20% La content after 1250 °C/4 h sintering [27]. All of these studies show that less La content makes the grain growth easier at the same sintering temperature.

Fig. 5 shows XRD profiles of LSFO ceramics prepared by the reaction-sintering process. It can be easily found that all peaks match with the ICDD PDF #01-082-1963 standard pattern of $(La_{0.4}Sr_{0.6})FeO_3$. LSFO ceramics could be obtained successfully by a simple process with the calcining stage bypassed. Density values of LSFO sintered at various temperatures are shown in Fig. 6. For LSFO with $x = 0.2$, density is not affected obviously by the sintering temperature. It increased with sintering temperature and reached a maximum

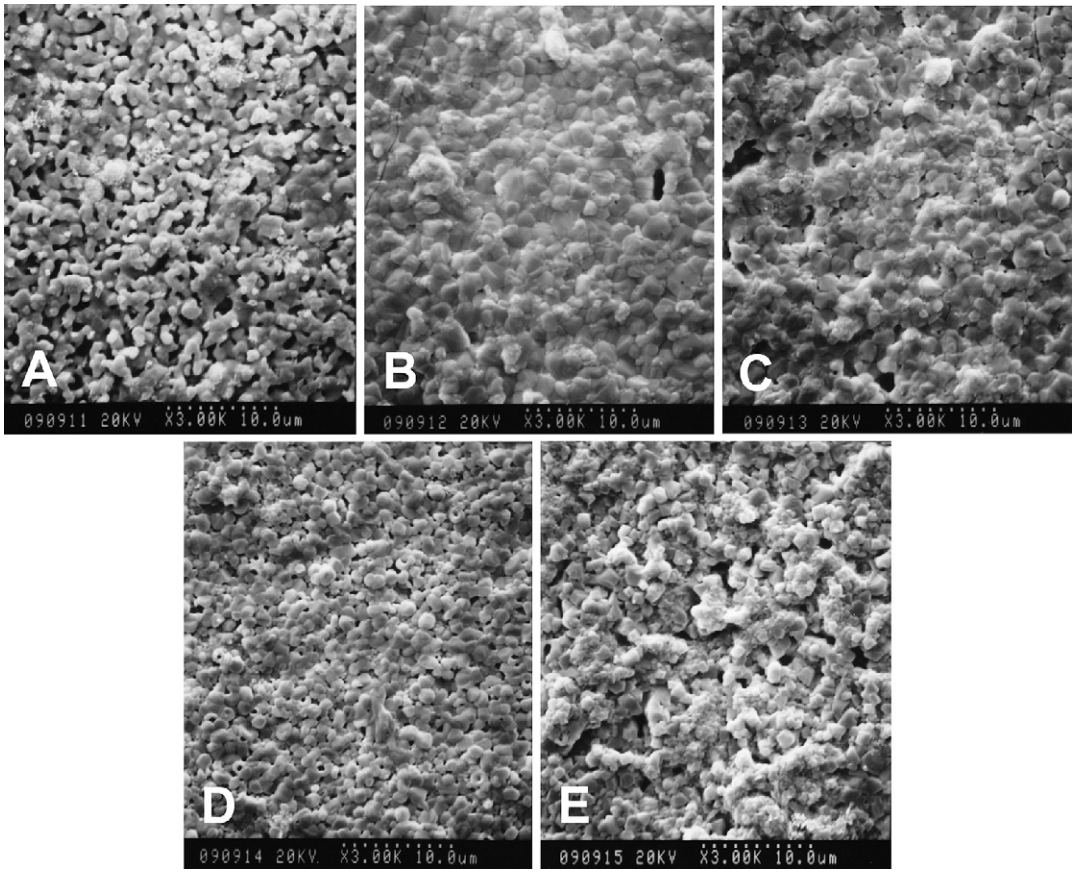

Fig. 4. SEM photographs of the as-fired $(La_xSr_{1-x})MnO_3$ ceramics with (A) $x = 0.2$, (B) $x = 0.25$, (C) $x = 0.3$, (D) $x = 0.35$ and (E) $x = 0.4$ after 1380 °C/2 h sintering.

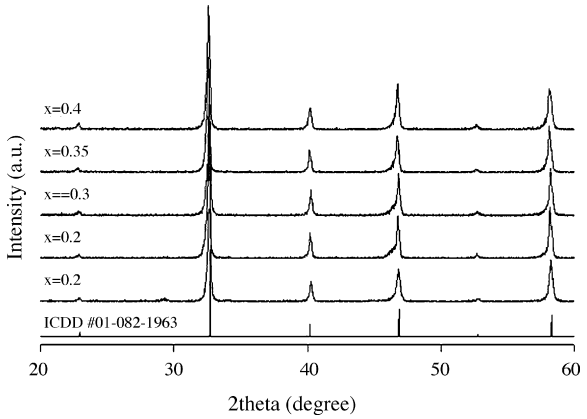

Fig. 5. XRD profiles of LSFO ceramics sintered at 1200 °C for 2 h.

value at 1230 °C. More La content resulted in a higher density at high sintering temperatures. The maximum density for LSFO with $x = 0.4$ is observed at 1250 °C. It implies that the temperature for densification in LSFO increases with increasing La content. Sintering temperature for LSFO is 150 °C lower than LSMO ceramics by a reaction-sintering process as shown in Fig. 2.

SEM photographs of as-fired LSFO ceramics sintered at 1230 °C/4 h are shown in Fig. 7. Very few pores were formed in these LSFO ceramics. This means that 1230 °C/4 h sintering is high enough for grain growth and densification in LSFO

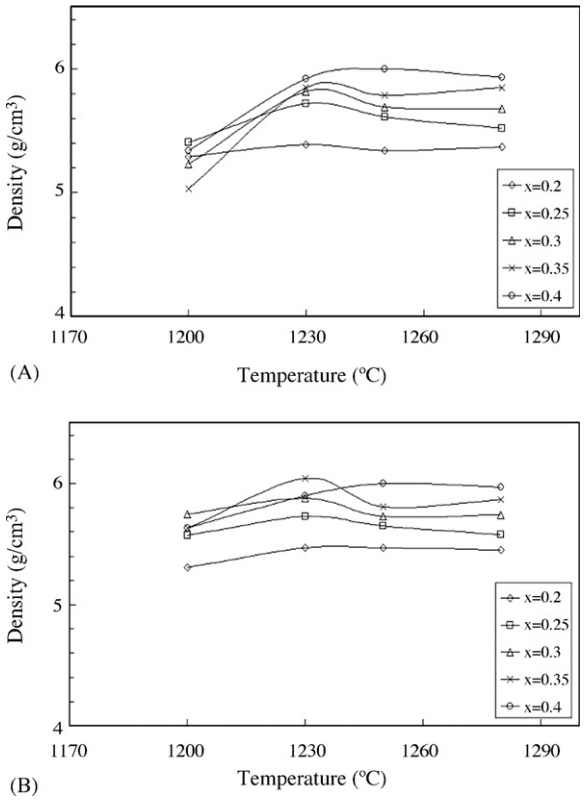

Fig. 6. Density of LSFO ceramics sintered at various temperatures for (A) 2 h and (B) 4 h.

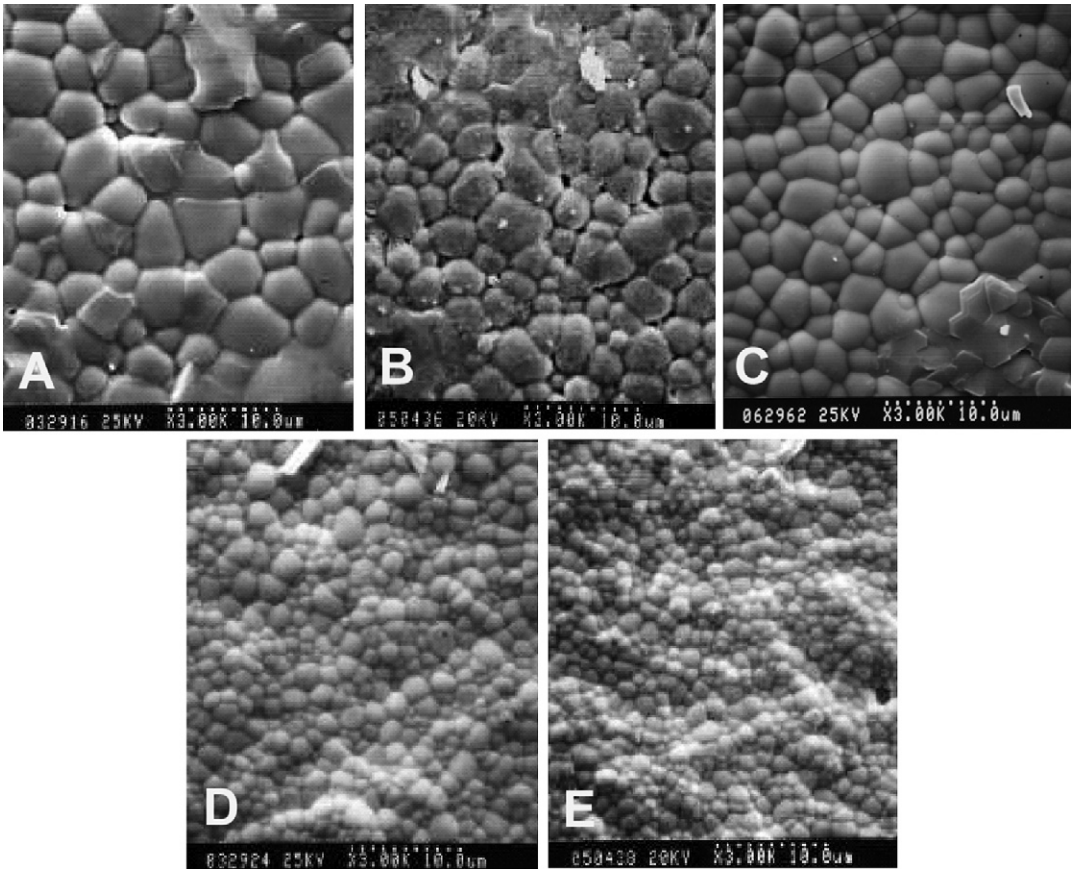

Fig. 7. SEM photographs of the as-fired $(La_xSr_{1-x})FeO_3$ ceramics with (A) $x = 0.2$, (B) $x = 0.25$, (C) $x = 0.3$, (D) $x = 0.35$ and (E) $x = 0.4$ after 1350 °C/2 h sintering.

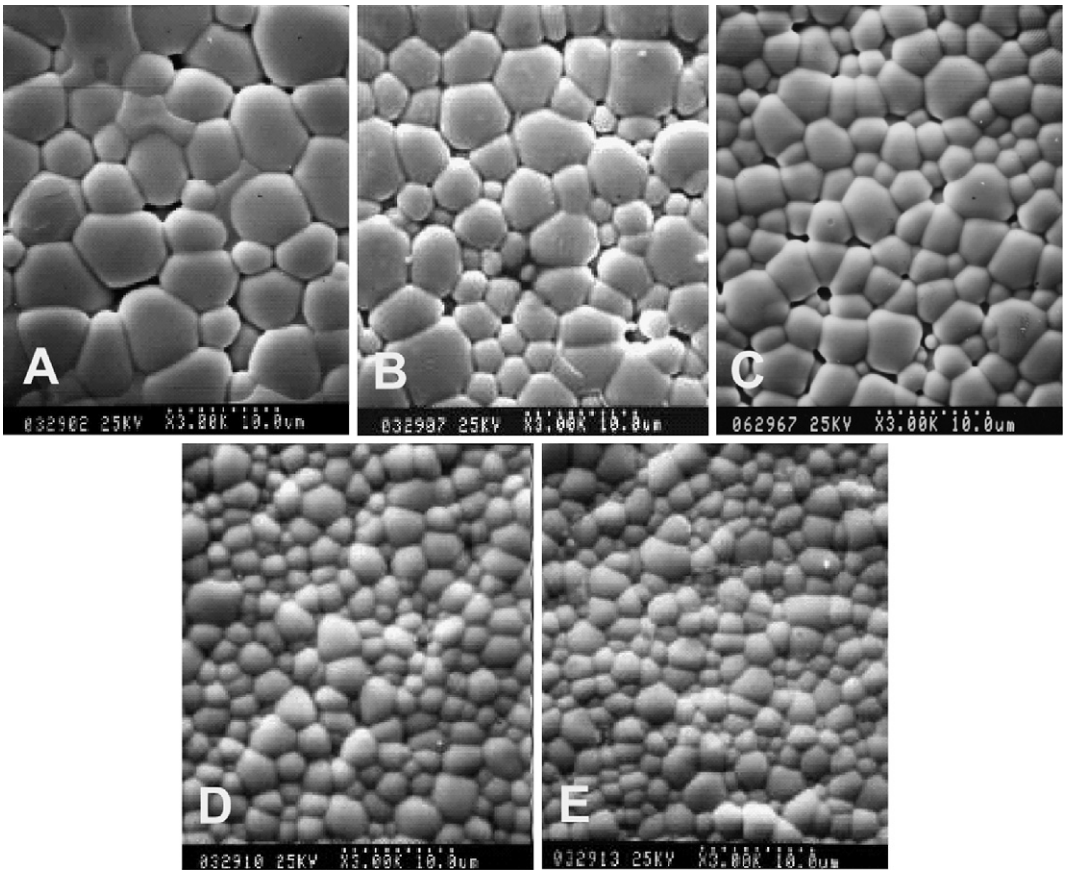

Fig. 8. SEM photographs of the as-fired $(La_xSr_{1-x})FeO_3$ ceramics with (A) $x = 0.2$, (B) $x = 0.25$, (C) $x = 0.3$, (D) $x = 0.35$ and (E) $x = 0.4$ after 1380 °C/2 h sintering.

ceramics prepared by the reaction-sintering process. It can be easily observed that the grain size of LSFO decreased as the La content increased. Similar tendency were observed in LSFO ceramics prepared by the conventional mixed oxide route [26]. SEM photographs of the as-fired LSFO ceramics sintered at 1250 °C/4 h are illustrated in Fig. 8. Pores are found in LSFO ceramics with $x = 0.2$ and 0.25. Similar results were found in LSFO by the conventional mixed oxide route [26]. Pores are not found in LSFO ceramics with $x = 0.35$ and 0.4. Grains of 6.95 μm for $x = 0.2$ and 3.37 μm for $x = 0.4$ were observed in LSFO ceramics sintered at 1250 °C/4 h. This is larger than LSFO ceramics prepared by the conventional route [26]. In LSFO ceramics prepared by the conventional route, 6.1 μm grains were formed for $x = 0.2$ and 2.4 μm for $x = 0.4$ at 1250 °C/4 h sintering [26].

4. Conclusion

LSMO and LSFO ceramics could be effectively obtained by a simple process with the calcining stage bypassed. Density increases with sintering temperature and reaches a maximum value at 1380 °C in 2 h sintering LSMO. The maximum density occurred at 1400 °C for 4 h sintering LSMO with $x = 0.35$ and 0.4. Sintering temperature for LSFO is about 150 °C lower than LSMO ceramics. Grain size decreased as La content increased in LSMO and LSFO ceramics. This is the same as in LSMO and LSFO ceramics prepared by conventional mixed oxide route. Larger grains were formed in LSMO and LSFO prepared by the reaction-sintering process than by the conventional mixed oxide route.

Acknowledgement

The authors are grateful to Miss Shi-Yuea Hsu for her help in obtaining the SEM photos.

References

[1] N.Q. Minh, High temperature fuel cells. Part 2. The solid oxide cell, CHEMTECH 21 (1991) 120–126.
[2] T. Yoshida, T. Hoshina, I. Mukaizawa, S. Sakurada, Properties of partially stabilized zirconia fuel cell, J. Electrochem. Soc. 136 (1989) 2604–2606.
[3] A.V. Virkar, Theoretical analysis of solid oxide fuel cells with two layers composite electrolytes: electrolyte stability, J. Electrochem. Soc. 138 (1991) 1481–1487.
[4] N.Q. Minh, Ceramic fuel cells, J. Am. Ceram. Soc. 76 (1993) 563–588.
[5] H. Obayashi, T. Kudo, Properties of oxygen-deficient perovskite-type compounds and their use as alcohol sensors, Nippon Kagaku Kaishi (1980) 1568–1572.
[6] W.B. Li, H. Yoneyama, H. Tamura, Studies on semiconductor gas sensors. III. Correlation between catalytic activity for carbon monoxide oxidation and sensor response to CO of $LaFeO_3$ and related perovskite oxides, Nippon Kagaku Kaishi (1982) 761–767.
[7] T. Inoue, N. Seki, K. Eguchi, H. Arai, Low-temperature operation of solid electrolyte oxygen sensors using perovskite-type oxide electrodes and cathodic reaction kinetics, J. Electrochem. Soc. 137 (1990) 2523–2527.

[8] Y. Shimizu, M. Shimabukuro, H. Arai, T. Seiyama, Enhancement of humidity sensitivity for perovskite-type oxides having semiconductivity, Chem. Lett. (1985) 917–920.
[9] P. Holtappels, C. Bagger, Fabrication and performance of advanced multilayer SOFC cathodes, J. Eur. Ceram. Soc. 22 (2002) 41–48.
[10] Y. Teraoka, H.M. Zhang, K. Okamoto, N. Yamazoe, Mixed ionic-electronic conductivity of $La_{1-x}Sr_xCo_{1-y}Fe_yO_{3-\delta}$ perovskite type oxides, Mater. Res. Bull. 23 (1988) 51–58.
[11] K. Huang, M. Feng, J.B. Goodenough, M. Schmerling, Characterization of Sr-doped $LaMnO_3$ and $LaCoO_3$ as cathode materials for a doped $LaGaO_3$ ceramic fuel cell, J. Electrochem. Soc. 143 (1996) 3630–3636.
[12] C.Y. Tsai, A.G. Dixon, Y.H. Ma, W.R. Moser, M.R. Pascucci, Dense perovskite $La_{1-x}A'_xFe_{1-y}Co_yO_{3-\delta}$ (A′ = Ba, Sr, Ca) membrane synthesis, applications, and characterization, J. Am. Ceram. Soc. 81 (6) (1998) 1437–1444.
[13] C.C. Chen, M.M. Nasralla, H.U. Anderson, M.A. Alim, Immittance response of $La_{0.6}Sr_{0.4}Co_{0.2}Fe_{0.8}O_3$ based electrochemical cells, J. Electrochem. Soc. 142 (2) (1995) 491–496.
[14] S. Bilger, E. Syskakis, A. Naoumidis, H. Nickel, Sol–gel synthesis of strontium-doped lanthanum manganite, J. Am. Ceram. Soc. 75 (4) (1992) 964–970.
[15] F. Licci, G. Turilli, P. Ferro, A. Ciccarone, Low temperature synthesis and properties of $LaMnO_{3+d}$ and $La_{0.67}R_{0.33}MnO_{3+d}$ (R = Ca, Sr, Ba) from citrate precursors, J. Am. Ceram. Soc. 86 (3) (2003) 413–419.
[16] Q. Zhang, T. Nakagawa, F. Saito, Mechanochemical synthesis of $La_{0.7}Sr_{0.3}MnO_3$ by grinding constituent oxides, J. Alloys Compd. 308 (2000) 121–125.
[17] S.P. Simner, M.D. Anderson, J.W. Stevenson, La(Sr)FeO_3 SOFC cathodes with marginal copper doping, J. Am. Ceram. Soc. 87 (8) (2004) 1471–1476.
[18] J.H. Chen, Y.C. Liou, K.H. Tseng, Stoichiometric perovskite lead magnesium niobate ceramics produced by reaction-sintering process, Jpn. J. Appl. Phys. 42 (1A) (2003) 175–181.
[19] Y.C. Liou, C.Y. Shih, C.H. Yu, Stoichiometric $Pb(Fe_{1/2}Nb_{1/2})O_3$ perovskite ceramics produced by reaction-sintering process, Mater. Lett. 57 (2003) 1977–1981.
[20] Y.C. Liou, C.T. Wu, K.H. Tseng, T.C. Chung, Synthesis of $BaTi_4O_9$ ceramics by reaction-sintering process, Mater. Res. Bull. 40 (9) (2005) 1483–1489.
[21] Y.C. Liou, J.H. Chen, H.W. Wang, C.Y. Liu, Synthesis of $(Ba_xSr_{1-x})(Zn_{1/3}Nb_{2/3})O_3$ ceramics by reaction-sintering process and microstructure, Mater. Res. Bull. 41 (3) (2006) 455–460.
[22] Y.C. Liou, W.H. Shiue, C.Y. Shih, Microwave ceramics $Ba_5Nb_4O_{15}$ and $Sr_5Nb_4O_{15}$ prepared by a reaction-sintering process, Mater. Sci. Eng. B 131 (2006) 142–146.
[23] Y.C. Liou, M.H. Weng, C.Y. Shiue, $CaNb_2O_6$ ceramics prepared by a reaction-sintering process, Mater. Sci. Eng. B 133 (2006) 14–19.
[24] Y.C. Liou, C.Y. Shiue, Preparation of $NiNb_2O_6$ columbite ceramics by a reaction-sintering process, Mater. Res. Soc. Symp. Proc. 848 (2005) 115–119.
[25] Y.C. Liou, Microstructure development in $(La_xSr_{1-x})MnO_3$ ceramics, Mater. Sci. Eng. B 108 (3) (2004) 278–280.
[26] Y.C. Liou, Effect of strontium content on microstructure in (La_xSr_{1-x})-)FeO_3 ceramics, Ceram. Int. 30 (5) (2004) 667–669.
[27] Y.S. Chou, J.W. Stevenson, T.R. Armstrong, L.R. Pederson, Mechanical properties of $La_{1-x}Sr_xCo_{0.2}Fe_{0.8}O_3$ mixed-conducting perovskites made by the combustion synthesis technique, J. Am. Ceram. Soc. 83 (6) (2000) 1457–1464.